

The MYB80 Transcription Factor Is Required for Pollen Development and the Regulation of Tapetal Programmed Cell Death in *Arabidopsis thaliana*

Huy Anh Phan, Sylvana Iacuone, Song F. Li, and Roger W. Parish¹

Botany Department, La Trobe University, Melbourne, Victoria 3086, Australia

Arabidopsis thaliana MYB80 (formerly MYB103) is expressed in the tapetum and microspores between anther developmental stages 6 and 10. MYB80 encodes a MYB transcription factor that is essential for tapetal and pollen development. Using microarray analysis of anther mRNA, we identified 404 genes differentially expressed in the *myb80* mutant. Employing the glucocorticoid receptor system, the expression of 79 genes was changed when MYB80 function was restored in the *myb80* mutant following induction by dexamethasone. Thirty-two genes were analyzed using chromatin immunoprecipitation, and three were identified as direct targets of MYB80. The genes encode a glyoxal oxidase (GLOX1), a pectin methylesterase (VANGUARD1), and an A1 aspartic protease (UNDEAD). All three genes are expressed in the tapetum and microspores. Electrophoretic mobility shift assays confirmed that MYB80 binds to all three target promoters, with the preferential binding site containing the CCAACC motif. TUNEL assays showed that when UNDEAD expression was silenced using small interfering RNA, premature tapetal and pollen programmed cell death occurred, resembling the *myb80* mutant phenotype. UNDEAD possesses a mitochondrial targeting signal and may hydrolyze an apoptosis-inducing protein(s) in mitochondria. The timing of tapetal programmed cell death is critical for pollen development, and the MYB80/UNDEAD system may regulate that timing.

INTRODUCTION

The tapetum forms a cell layer surrounding developing microspores within the anther locule. In *Arabidopsis thaliana*, tapetal cells are derived from primary sporogenous cell lineages during anther developmental stage 4 (Sanders et al., 1999). During microspore development, the tapetum supplies necessary nutrients and structural components. As the pollen matures, the tapetum undergoes programmed cell death (PCD), releasing tapetal remnants, including elaioplasts and tapetosomes, which are incorporated into the coat of mature pollen grains (Wu et al., 1997; Hsieh and Huang, 2007; Parish and Li, 2010). Tapetal PCD is a highly orchestrated event that occurs synchronously with pollen mitotic division and formation of the exine coat (Sanders et al., 1999). Tapetal degeneration begins at stage 10 and is completed by stage 11. Tapetal PCD appears to be apoptosis like, as it is relatively rapid and possesses characteristic features of apoptosis, such as chromatin condensation, DNA fragmentation, and mitochondrial and cytoskeletal disintegration (Papini et al., 1999; Love et al., 2008).

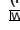
Transcription factors known to be involved in tapetal development include DYSFUNCTIONAL TAPETUM1 (*DYT1*) (Zhang et al., 2006), MYB33/MYB65 (Millar and Gubler, 2005), DEFECTIVE IN TAPETAL DEVELOPMENT AND FUNCTION1 (*TDF1*) (Zhu et al.,

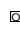
2008), ABORTED MICROSPORES (*AMS*) (Sorensen et al., 2003), MALE STERILITY1 (*MS1*) (Wilson et al., 2001; Ito and Shinozaki, 2002) and MYB80 (formerly MYB103) (Higginson et al., 2003; Li et al., 2007; Zhang et al., 2007). *DYT1* and *AMS* both encode basic-helix-loop-helix proteins, whereas *TDF1* and *MS1* encode MYB and PHD transcription factors, respectively. The *dyt1*, *tdf1*, and *ams* mutants exhibit a similar tapetal defect, namely, increased vacuolation and enlargement of the tapetum resulting in arrested microspore development. Transcript levels of *AMS*, *MYB80*, and *MS1* are significantly reduced in the *dyt1* mutant, suggesting that they act downstream of *DYT1* (Zhang et al., 2006). Based on analysis of transcript levels within *tdf1* and *ams* mutants, Zhu et al. (2008) suggested that *TDF1* functions upstream of *AMS* and that *AMS* is upstream of *MYB80*. Xu et al. (2010) identified 13 genes as direct targets of *AMS* using chromatin immunoprecipitation, but *MYB80* was not among them. Transcript levels of *MS1*, *MS2*, and *A6* are downregulated in the *myb80* mutant, suggesting they act downstream of *MYB80* (Zhang et al., 2007). It is not known if the three genes are directly or indirectly regulated by MYB80.

MYB80 was isolated from an *Arabidopsis* genomic library using degenerate primers covering a conserved region within the third repeat of several MYB genes (Li et al., 1999). *MYB80* expression is clearly detected in the tapetum and microspores of anthers containing tetrads (stage 7), and expression persists until stage 10 when the tapetum begins to degenerate (Higginson et al., 2003; Li et al., 2007). Functional disruption of *MYB80* using antisense (Higginson et al., 2003), T-DNA knockout (Li et al., 2007), or point mutation (Zhang et al., 2007) resulted in a partial (in the case of the antisense lines) or complete male sterility. The *myb80* mutant exhibits signs of premature tapetal degeneration in stage 6 anthers, which becomes more pronounced at stage 7,

¹ Address correspondence to r.parish@latrobe.edu.au.

The author responsible for distribution of materials integral to the findings presented in this article in accordance with the policy described in the Instructions for Authors (www.plantcell.org) is: Roger W. Parish (r.parish@latrobe.edu.au).

 Online version contains Web-only data.

 Open Access articles can be viewed online without a subscription. www.plantcell.org/cgi/doi/10.1105/tpc.110.082651

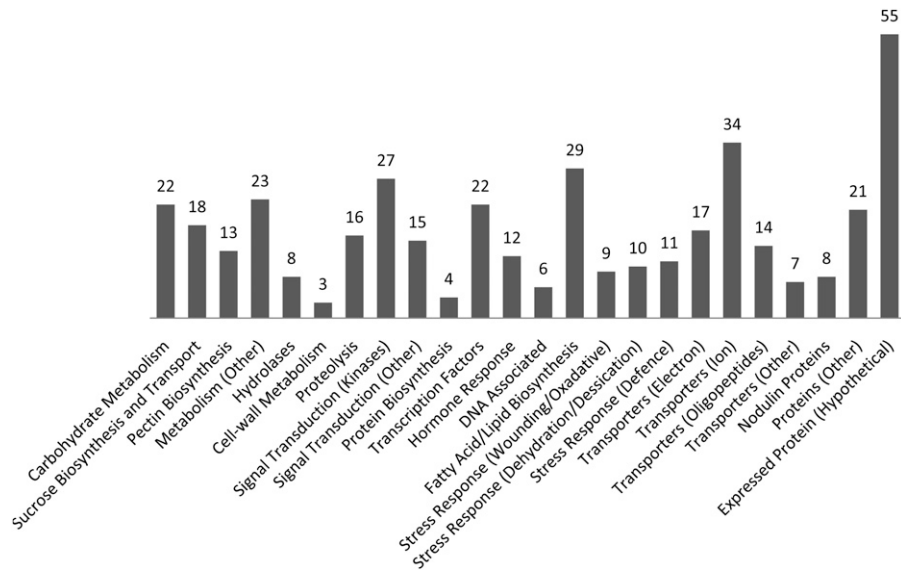


Figure 1. Genes That Are Differentially Expressed in *myb80* Mutant Anthers.

The genes are categorized into groups based on known and predicted functions. The data consist of genes that have a fold change between 2 and 17 and a P value <0.02. The most highly represented biological function groups includes transporters (19%), metabolism (12%), signal transduction components (11%), fatty acid/lipid biosynthesis (7%), and transcription factors (5%). The complete list is presented in Supplemental Data Set 1 online.

where an increase in tapetal vacuolation occurs. At stage 7, the tapetal cell wall does not degrade in the mutant, suggesting that the transition to a secretory tapetum fails to occur. The release of tetrads, which requires callose dissolution by enzymes secreted from the tapetum, is significantly reduced in the *myb80* mutant. Expression of *A6*, a gene encoding for a putative callase resembling β 1,3-glucanases, is reduced in the mutant (Zhang et al., 2007).

Here, microarray analysis identified 404 genes showing differential expression in young anthers of the *myb80* mutant compared with wild-type anthers. To narrow down the number of candidate target genes, an inducible system using dexamethasone as the inducer of an *AtMYB80:glucocorticoid receptor (GR)* construct was used to restore fertility in the *myb80* mutant. After 24 h of DEX treatment, the expression levels of 79 genes were significantly changed in anthers. Thirty-two were selected for chromatin immunoprecipitation (ChIP) analysis and three found to be directly regulated by MYB80. The in vitro DNA binding specificity and anther expression patterns were examined. Two of the genes, encoding a pectin methyltransferase and a glyoxal oxidase, appeared to be downregulated by MYB80, while the third gene, encoding an A1 aspartic protease, was upregulated. When the latter was silenced using small interfering RNA (siRNA), TUNEL assays showed that premature tapetal and microspore cell death

occurred, a phenotype resembling the *myb80* mutant. Consequently, we named the aspartic protease gene *UNDEAD*. *UNDEAD* has a mitochondrial targeting signal, and the MYB80/*UNDEAD* system may regulate the timing of tapetal PCD.

RESULTS

Identification of MYB80 Downstream Genes Using Microarray Analysis of *myb80* versus Wild-Type Anthers

In order to identify the genes regulated by MYB80, microarray technology was employed to analyze the expression levels of genes that were differentially regulated in the *myb80* mutant when compared with wild-type anthers. Approximately 1000 anthers at stages 5 to 8 were dissected from the wild type and the *myb80* mutant for each biological replicate for subsequent RNA isolation, labeling, and hybridization to Affymetrix *Arabidopsis* ATH1 genome arrays. In the microarray analysis, 404 genes were differentially expressed by >2-fold in the *myb80* mutant compared with the wild type and possessed a P value of <0.02. The data set included 297 genes that were downregulated in *myb80* and 107 genes that were upregulated, with differential gene expression ranging from 2- to 17-fold.

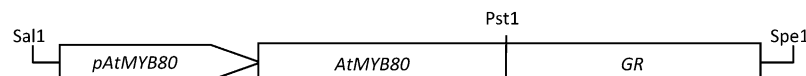


Figure 2. Schematic Diagram of the *AtMYB80:GR*-Inducible Construct.

The construct consists of 1104 bp of *MYB80* promoter sequence and 1471 bp of coding sequence fused to 1.5 kb of the *GR* gene in the pCambia 1380 vector. Restriction enzymes used in the cloning process are indicated above the construct.

Genes were categorized according to known or putative function based on gene ontology annotations obtained from Affymetrix. Differentially expressed genes included those involved in a variety of biological processes, such as signal transduction, carbohydrate metabolism, transport, lipid and fatty acid metabolism, and Suc metabolism along with several transcription factors and genes involved in ion transport (Figure 1). The complete list is presented in Supplemental Data Set 1 online.

Eight genes were selected from the data set for verification of the microarray data. These genes were selected on the basis of high differential expression and low P values. RT-PCR analysis correlated with results obtained in the microarray experiment (see Supplemental Figure 1 online).

Ten genes were selected for further analysis based on substantial changes in gene expression in the *myb80* mutant and low P values. T-DNA insertion mutants were obtained for each of the selected genes as summarized in Supplemental Table 1 online. Plants homozygous for the T-DNA were examined for any phenotypic changes in pollen morphology and tested for pollen viability by Alexander's staining. There were no distinguishable phenotypic changes in the homozygous mutants when compared with the wild type, and male fertility was unaffected. This indicates that the genes examined are redundant or are not direct targets of MYB80.

The *myb80* T-DNA mutant is characterized by premature degradation of the tapetum and pollen grains. Hence, it is probable that many of the genes observed in the microarray data set were differentially expressed as a consequence of tapetal breakdown rather than a direct result of eliminating functional MYB80 protein.

Microarray Analysis of AtMYB80:GR-Inducible Lines

To facilitate the identification of MYB80 target genes, an inducible system was employed. The GR domain was fused to the C terminus of MYB80 and the construct driven by the endogenous

MYB80 promoter (Figure 2). This construct was transformed into *myb80* mutant plants. Following application of dexamethasone (DEX), the AtMYB80:GR fusion protein is able to enter the nucleus, resulting in complete restoration of male fertility (Li et al., 2007). Comparison of gene expression levels just prior to and following application of DEX was expected to enable identification of MYB80 target genes.

Postfunctional MYB80 protein induction was examined using microarray analysis. Treatments included pre-DEX (noninduced) and 3 to 5 h, 8 to 10 h, and 24 h post-DEX induction. Each time course consisted of four biological replicates. Three biological replicates of *myb80* mutants at 8 to 10 h post-DEX (MT) were included as a control. Each replicate contained RNA extracted from ~1000 developmental stage 5 to 8 anthers. Analysis of data obtained from the 3 to 5 h and 8 to 10 h post-DEX samples when compared with pre-DEX and/or the *myb80* 8 to 10 h control samples revealed only minor differential gene expression changes, with all the genes showing a change of <2-fold. This suggests that 3 to 5 h and 8 to 10 h DEX exposure is insufficient for downstream gene induction to occur.

The 24 h post-DEX induction microarray data sets were separately analyzed as two groups to identify overlap. Group A consisted of the pre-DEX and *myb80* mutant (MT) data sets versus 24-h post-DEX (Dex24). Group B consisted of wild-type versus pre-DEX and *myb80* (MT) mutant data sets. Group A reflects gene expression changes seen in anthers as they transition from male sterility to full fertility after MYB80 induction. Group B represents differences in gene expression between the wild type and the pre-DEX (noninduced) and *myb80* mutant. The genes shared by the two comparisons reflect the subset of genes most likely to be directly regulated by MYB80 (Figure 3). The overlapping data set consists of 79 genes that were differentially expressed by 2- to 87-fold with corresponding P values of <0.02 (see Supplemental Table 2 online).

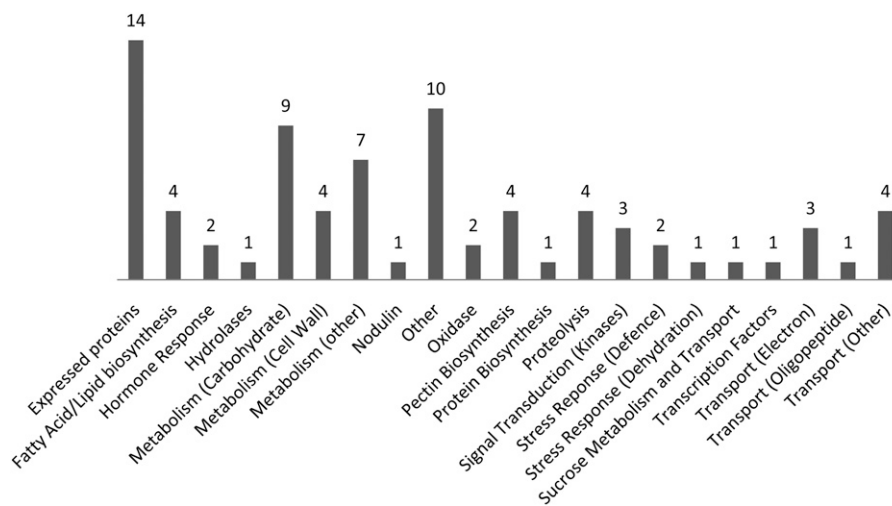


Figure 3. Genes That Are Differentially Expressed 24 h Postfunctional MYB80 Induction.

The genes were categorized into groups based on known and predicted functions. The data consist of genes that have a fold change between 2 and 87 and a P value <0.02. The highest represented biological function groups include metabolism (25%), transporters (10%), fatty acid/lipid biosynthesis (5%), pectin biosynthesis (5%), and proteolysis (5%). The complete data set is presented in Supplemental Table 2 online.

In order to verify the microarray data and identify genes directly downstream of MYB80, RT-PCR analysis of nine genes selected on the basis of low P values was conducted over a time course including pre-DEX plus 10, 24, 48, and 72 h post-DEX (see Supplemental Figure 2 online). All RNA samples were extracted from young anthers at developmental stages 5 to 8. RT-PCR analysis showed that the transcript levels of four genes, including At3g11980, At1g01280, At4g22080, and At1g66460, were induced in young anthers 24 h after the application of DEX. Expression levels peaked at either 48 or 72 h. Low levels of At1g02050 and At4g12920 transcripts were observed pre-DEX. Expression increased at 24 h post-DEX and peaked at 48 or 72 h post-DEX for At4g12920 and At1g02050, respectively. These results are consistent with the microarray data analysis. Twelve additional genes were analyzed using T-DNA insertion mutants;

however, all exhibited wild-type pollen development and seed set (see Supplemental Table 1 online).

ChIP Identifies Three MYB80 Direct Target Genes

To identify directly regulated downstream genes, ChIP was employed. Saleh et al. (2008) successfully achieved enrichment of specific targets using ~0.2 g of plant material. Hence, we performed ChIP using this protocol with some modifications, in particular, the use of young floral buds and dissected anthers rather than whole seedlings. To enrich for the AtMYB80:GR complex, the anti-GR antibody PA1-516 was used. Twenty-eight genes were selected from the 24 h postinduction microarray data set for the ChIP assay (Table 1). The criteria for selection included stamen-specific expression, although gene function was the key

Table 1. A Subset of Genes from the Inducible MYB80 Microarray Data Set Analyzed by ChIP

Gene Locus ID	Name or Annotation	Predicted MYB Binding Motifs	Dex24	ChIP
At4g12920	Aspartic protease/UNDEAD	MYB1AT x8, MYBST1 x3, MYB1LEPR x2, MYBGAHV	14.67	+
At1g67290	Glyoxal oxidase/GLOX1	MYB1AT, MYBPZM	-2.91	+
At2g47040	PME/VANGUARD1	MYB1AT x4, MYBCORE, MYBGAHV, MYBST1	-29.19	+
At1g01280	Cytochrome p450	MYBCORE x2, MYBGAHV x3, MYB1LEPR	87.68	-
At1g02790	Polygalacturonase 4	MYBCORE, MYBGAHV x2	-21.22	-
At1g02930	Glutathione S-transferase, putative	MYB1AT x2, MYBGAHV, MYBST1, MYB1LEPR, MYBCOREATCYCB1	-2.62	-
At1g29270	Expressed protein	MYB1AT	13.14	-
At1g54540	late embryogenesis abundant (LEA)	MYB1AT, MYBCORE	10.16	-
At1g78140	Methyltransferase	MYB1AT x3, MYBST1	2.08	-
At2g02810	UDP-galactose transporter 1	MYB1AT x3, MYBCOREATCYCB1	2.53	-
At2g03740	LEA	MYB1AT, MYBGAHV x2, MYB1LEPR	2.15	-
At2g42570	Expressed protein	MYB1AT x3	2.90	-
At2g43520	Trypsin inhibitor, putative	MYB1AT x2, MYBGAHV	2.16	-
At2g46660	Cytochrome p450, putative	MYB1AT, MYBST1, MYBCOREATCYCB1	2.6	-
At2g47050	Invertase/PME inhibitor	MYB1AT x2, MYBCORE	-8.85	-
At3g01700	Arabinogalactan protein 11	MYBST1	-3.41	-
At3g01290	Band 7 family protein	MYB1AT, MYBST1	-2.13	-
At3g02480	LEA, abscisic acid-responsive protein	MYB1AT, MYBCORE x2, MYBST1, MYBGAHV	-5.27	-
At3g11980	Male Sterility2 (MS2)	MYB1AT x3, MYBGAHV x2, MYB1LEPR	24.85	-
At3g23770	Glycosyl hydrolase	MYB1AT, MYBCORE, MYB1LEPR, MYBPZM	37.49	-
At3g62180	PME	MYBCORE, MYBGAHV, MYBCOREATCYCB1 x2, MYBPZM	-2.25	-
At4g11760	Pollen coat protein	MYB1AT x2, MYBCORE x2, MYBGAHV	-11.75	-
At4g14080	A6, putative callase/MEE48	MYBPZM	<2	-
At4g16160	Inner membrane translocase	MYBCORE, MYBST1, MYBCOREATCYCB1 x2	-4.27	-
At4g22080	Pectate lyase		14.7	-
At4g30030	Aspartic protease	MYB1AT, MYBCORE x2	N/A	-
At4g30040	Aspartic protease	MYB1AT, MYBST1	9.85	-
At5g09550	Rab GDP dissociation inhibitor	MYB1AT, MYBCORE x2, MYBCOREATCYCB1	-7.65	-
At5g52160	Protease inhibitor	MYBST1	5.97	-
At5g22260	Male Sterility 1 (MS1)		N/A	-
At5g48880	Acetyl-CoA C-acyltransferase 1	MYBCORE, MYBST1 x2	3.23	-
At5g56110	MYB80/MYB103	MYBST1, MYBGAHV x2, MYBPZM	<2	-

Predicted MYB binding motifs present in the promoters (up to -600 bp from the ATG) were obtained using cis-PLACE analysis. ChIP identified *UNDEAD*, *GLOX1*, and *VGD1* as direct targets of MYB80. The aspartic protease At4g30030 was examined by ChIP as it occurs in tandem with At4g0040. *MS1* is absent from the Affymetrix ATH1 array. A6 and *MYB80* transcript difference was <2-fold. Dex24, differential gene expression (fold change) 24 h postfunctional MYB80 induction. MYB1AT, A/TAACCA (Abe et al., 2003); MYBCORE, CNGTTA/G (Urao et al., 1993); MYBST1, GGATA (Baranowskij et al., 1994); MYBGAHV, TAACAAA (Gubler et al., 1999); MYB1LEPR, GTTAGTT (Chakravarthy et al., 2003); MYBCOREATCYCB1, AACGG (Planchais et al., 2002); MYBPZM, CCA/TACC (Grotewold et al., 1994). N/A, not present on the ATH1 array. Primers are presented in Supplemental Table 5 online.

determinant. Three of these genes are known to be involved in male fertility, namely, *VANGUARD1* (*VGD1*) (At2g47040), *MALE STERILITY2* (At3g11980), and *CYTOCHROME P450* (At1g01280) (Aarts et al., 1993; Jiang et al., 2005; Morant et al., 2007). In addition, genes downstream of MYB80, such as *MALE STERILITY1* and *A6* (Zhang et al., 2007), were selected. Tandem genes, such as *At4g30030* (aspartic protease) and *At2g47050* (invertase/pectin methylesterase inhibitor), were also examined. The remaining genes on the list are proteases or participate in structural component biosynthesis. Proteases may function in tapetal and pollen development as many proteases were found to be downregulated in previous *ms1* and *ams* gene expression studies (Ito et al., 2007; Yang et al., 2007; Xu et al., 2010).

The promoters of the selected genes were analyzed for the presence of putative MYB binding elements immediately upstream of the TATA box transcription start site using the cis-PLACE (<http://www.dna.affrc.go.jp/PLACE>) database. PCR primers were designed to flank MYB binding elements to generate an amplicon of ~300 to 400 bp. All primers were tested by PCR using wild-type genomic DNA and sonicated ChIP samples as template.

Three out of the 32 genes analyzed were positively enriched in the +AB (antibody) compared with the –AB samples (Figure 4). These genes encode for *VGD1* (At2g47040), a glyoxal oxidase (At1g67290, named *GLOX1*), and an A1 aspartic protease (At4g12920, named *UNDEAD*). The remaining genes did not exhibit enrichment in the +AB samples and so are unlikely to be direct targets of MYB80 (see Supplemental Figures 3 and 4 online). *MS2*, *A6*, and *MS1* were not enriched. Hence, their downregulation in the *myb80* mutant (Zhang et al., 2007) may be a consequence of tapetal degeneration. Alternatively, the genes may be indirectly activated by MYB80. MYB80 does not appear to bind to its own promoter even though there are several MYB *cis*-elements present in the region immediately upstream of the TATA box.

MYB80 Directly Binds to MYB Binding *cis*-Elements Present in the Promoters of *VGD1*, *GLOX1*, and *UNDEAD*

To complement the ChIP results, electrophoretic mobility shift assays (EMSAs) were used to confirm binding to the target promoters by MYB80 and determine if any of the *cis*-elements were preferentially bound. Recombinant full-length and truncated MYB80 protein was expressed and purified from *Escherichia coli* (see Supplemental Figure 5 online). The full-length MYB80 protein was expressed at very low levels and so the truncated protein was used. The truncated MYB80 protein consists of the entire MYB domain and sequences up to the amino acids LLTKRV. Based on our work and other previous work, truncation of MYB proteins beyond the MYB domain does not appear to affect specificity (Ramsay et al., 1992; Li and Parish, 1995). Probes were generated using PCR to incorporate digoxigenin-labeled dUTP into the amplified product. As the consensus MYB80 binding motif was unknown, the probes were designed based on the promoter sequence targeted by the ChIP analysis and were ~170 to 180 bp in length containing one or more potential MYB binding motifs (Figures 5A to 5C). Sequence analysis identified three types of MYB binding motifs present in the probes, namely, MYBPZM (CC^A_TACC), MYB1AT

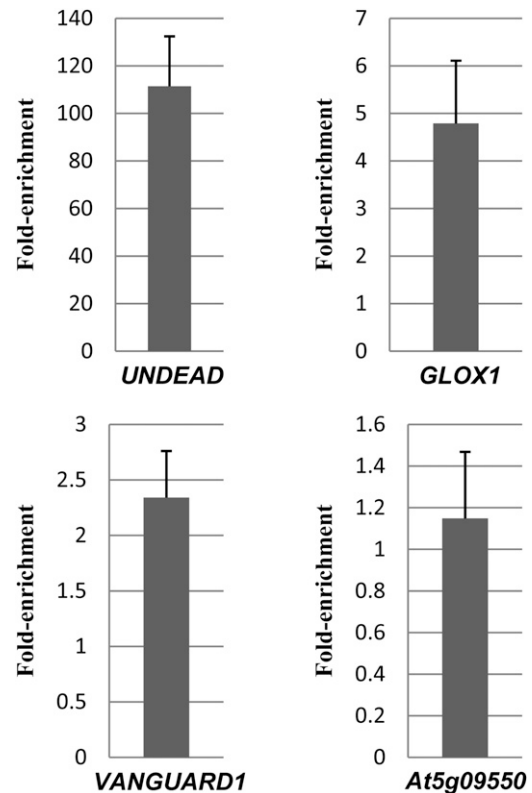


Figure 4. qChIP-PCR Analysis of Enrichment of MYB80 Target Genes in Floral Buds.

Fold enrichment represents the fold change in +AB (antibody) compared with –AB samples. qPCR data were gathered from two biological and three technical replicates. Error bars represent SD. qPCR data correlate with standard ChIP-PCR with *UNDEAD* strongly enriched, followed by moderate enrichment of *GLOX1* and weak enrichment of *VGD1* (see Supplemental Figures 3 and 4 online). *At5g09550* levels were not affected by the anti-GR PA-516 antibody, suggesting it is not a direct target.

(^A_TAACCA), and MYB1LEPR (GTTAGTT) (Grotewold et al., 1994; Abe et al., 2003; Chakravarthy et al., 2003). To identify the preferred binding sequence of MYB80, 30-bp unlabeled probes were generated to span the individual *cis*-elements and used as competitors.

MYB80 appears able to bind all three target gene promoters (Figures 5D to 5F); however, there are multiple shifts, which indicates either dimer formation or the binding of more than one protein molecule to the target probe. The latter is the more likely explanation as it has been demonstrated that c-Myb is able to bind multiple times to probes that contain more than one MYB binding site (Ramsay et al., 1992). The addition of competitor probes also reduced or abolished the multiple shifts, supporting multiple protein/DNA interactions rather than dimer formation. The MYB binding *cis*-elements present in the promoters of *UNDEAD*, *GLOX1*, and *VGD1* all share the same core sequence of AACCC with differences occurring in the adjacent nucleotides. AACCC forms the core of the MYB1AT *cis*-element bound by

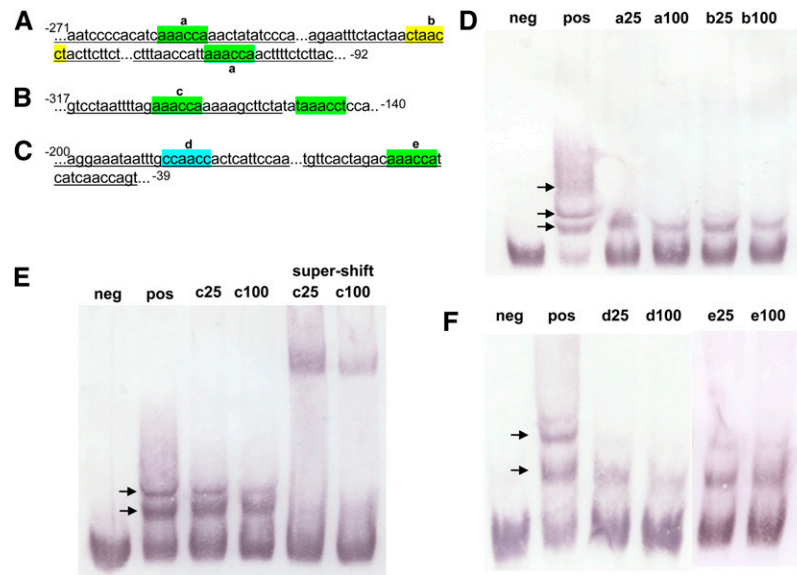


Figure 5. EMSA Shows MYB80 Is Able to Bind to the Promoter of All Three Target Genes at Several Different MYB Binding *cis*-Elements.

- (A) The *UNDEAD* probe contains three MYB binding *cis*-elements. Underlined sequences represent unlabeled competitors “a” and “b.”
- (B) The *VGD1* probe contains two MYB binding *cis*-elements with a single unlabeled competitor “c” underlined.
- (C) The *GLOX1* probe contains two MYB binding *cis*-elements. Underlined sequences are unlabeled competitors “d” and “e.” Numbers denote location relative to the ATG translational start site. Highlighted colors represent the motifs MYB1AT (green), MYB1LEPR (yellow), and MYBPZM (blue).
- (D) MYB80 is able to bind to all three *cis*-elements present in the *UNDEAD* promoter. Nonlabeled competitors are able to reduce the visible shift significantly (arrows), resulting in an increase in free probe.
- (E) MYB80 is able to bind to both MYB1AT *cis*-elements present in the *VGD1* promoter. The unlabeled “c” competitor even at 100-fold does not significantly reduce the second visible shift, suggesting GAAACCA is not the preferred motif. The reduction is more prominent in the supershift using a T7 antibody against the fusion MYB80 protein.
- (F) MYB80 preferentially binds to the MYBPZM *cis*-element (CCAACC) in the *GLOX1* promoter as “d” is the most effective competitor at reducing the visible shifts. neg, free labeled probe (no MYB80 protein); pos, labeled probe and MYB80; a-e/25/100, pos + unlabeled competitors at 25- and 100-fold compared with labeled probe.

MYB2 with a consensus sequence of CTAACCA (Abe et al., 1997). The least effective competitor contains the 5' nucleotide G adjacent to the core motif (Figures 5B and 5E). The most effective competitor probe contains a single MYBPZM *cis*-element (Figures 5C and 5F). MYB80 appears to have the highest binding affinity for the sequence CCAACCA, which is also the preferential binding site of the maize (*Zea mays*) P and C1 MYB proteins (Grotewold et al., 1994; Sainz et al., 1997).

Expression Analysis of the Target Genes

A positively regulated target gene should possess a similar expression pattern to *MYB80*, namely, expression in the tapetum and/or microspores from anther developmental stage 6 until stage 10. *MYB80* expression is absent in stage 11 anthers (Higginson et al., 2003; Li et al., 2007). Promoter:*GUS* (β -glucuronidase) constructs were created, and quantitative RT-PCR (qRT-PCR) analysis was performed to detect transcript levels of the three target genes and *MYB80* (see Supplemental Figure 6 online) in young floral buds (corresponding with anther stages 9 and below) and mature floral buds (anther stages 10 to 12).

The GUS staining pattern shows that the *UNDEAD* promoter is active specifically in anthers of young floral buds, with weak

expression present in stage 6 increasing at stage 7 to 9 anthers (see Supplemental Figure 7 online). Sections reveal strong GUS staining in the tapetal cell layer and in the developing microspores (Figures 6A to 6D). No GUS staining was observed in stage 11 and beyond, mirroring the expression pattern of *MYB80*. qRT-PCR detected high levels of *UNDEAD* transcript in young floral buds, but levels were significantly reduced in mature floral buds (Figure 6E).

The *GLOX1* promoter drives *GUS* expression within anthers of floral buds from stage 8 onwards with very strong GUS staining present in mature and released pollen grains (see Supplemental Figure 7 online). GUS staining was strongest in stage 10 anthers and persisted at high levels up to stage 14. Sections show strong GUS staining in the tapetum, developing microspores, and mature pollen grains from late stage 8 (Figures 7A and 7B). qRT-PCR detected low levels of *GLOX1* transcript in young floral buds but levels were significantly increased in mature floral buds (Figure 7C).

The microarray analysis suggests *VGD1* expression is strongly repressed by MYB80. Therefore, *VGD1* should not be expressed at high levels during early anther developmental stages where MYB80 is most active. Previously, Jiang et al. (2005) showed *VGD1* expression is specific to mature pollen grains and pollen

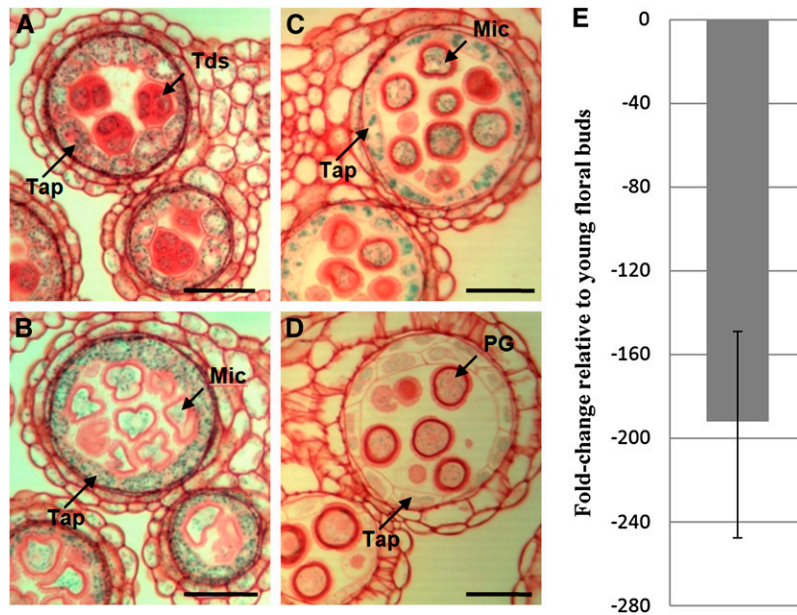


Figure 6. ASPARTIC PROTEASE/*UNDEAD* Expression Analysis.

(A) to (D) Sections (3 μm) of *UNDEAD* promoter:*GUS* anthers stained with safranin. Light microscopy of anthers at stages 7 (A), 8 (B), 9 (C), and early 10 (D) shows tapetum- and microspore-specific expression. Weak *GUS* activity is present in stage 10 pollen grains. No *GUS* activity was detected in stage 11 and beyond.

(E) Comparative qRT-PCR analysis of *UNDEAD* transcript levels in wild-type mature (anther stages 10 to 12) versus young (anther stages ≤ 9) floral buds. The *UNDEAD* transcript level is lower in mature floral buds. Error bar represents sd. Tap, tapetum; Tds, tetrads; Mic, microspores; PG, pollen grain. Bars = 25 μm .

tubes; however, there was no examination or mention of the tapetum. *GUS* staining shows the promoter of *VGD1* is active within the late tapetum and mature pollen grains. *GUS* staining was faint but present in stage 9 anthers and became progressively stronger in stage 10 anthers and beyond. Sections identified tapetum-specific expression occurring in stage 10 to 11 anthers where the tapetum is undergoing PCD but activity was predominantly in mature pollen grains (Figures 8A to 8D). qRT-PCR detected low levels of *VGD1* transcript in young floral buds but levels were significantly increased in mature floral buds (Figure 8E).

Functional Analysis of the Target Genes

The function of *VGD1*, encoding a pectin methylesterase, has been studied by Jiang et al. (2005). The *vgd1* mutant was isolated from enhancer-trap dissociation (*Ds*) insertion lines in *Arabidopsis* ecotype Landsberg *erecta* (Sundaresan et al., 1995). The homozygous mutant has smaller and shorter siliques with fewer seeds, and pollen tube growth in the style and transmitting tract is severely retarded. Tapetal cell development in the mutant was not examined, and *vgd1* pollen appeared morphologically normal (Jiang et al., 2005).

SALK_000947 seeds containing a T-DNA insertion in the first exon of *GLOX1* (Scholl et al., 2000; European Arabidopsis Stock Centre) were obtained and germinated on kanamycin germination medium. PCR confirmed the presence of the T-DNA in the 23

lines that survived selection. However, no homozygous *glox1* lines could be identified.

Gene silencing was used to downregulate *UNDEAD* transcript levels as no suitable insertion mutants are available. Three constructs were created using the endogenous *UNDEAD* promoter to drive two siRNAs and an artificial microRNA (amiRNA). The two siRNAs consisted of a short 21-nucleotide hairpin targeting the *UNDEAD* transcript at the nucleotide positions 121 and 297 (Figure 9A). The amiRNA (MIR319a backbone) also targeted the *UNDEAD* transcript at nucleotide position 121. The silencing vectors were transformed into wild-type *Arabidopsis* (Columbia-0), and over 30 transgenic lines were obtained for each construct. The majority (>70%) of transgenic siRNA-121 lines exhibited partial male sterility with reduced silique elongation and seed set. Both the siRNA-297 and amiRNA transgenic lines also displayed partial male sterility, but the majority (~75%) of lines were identical to the wild type.

Real-time qPCR was performed on young floral buds at stages 6 to 10 from three siRNA-121 lines selected for their varying degrees of partial male sterility (Figure 9B). Line #1 had less than half of the siliques elongating and had a full complement of seeds, whereas line #3 was severely male sterile with almost no seed set (Figure 9C). The endogenous *UNDEAD* promoter was effective in driving the siRNA as a reduction in *UNDEAD* transcript occurred in all three lines tested. Line #3 had the highest level of *UNDEAD* transcript silencing, with the mRNA level reduced by ~85% compared with the wild type. The qRT-PCR

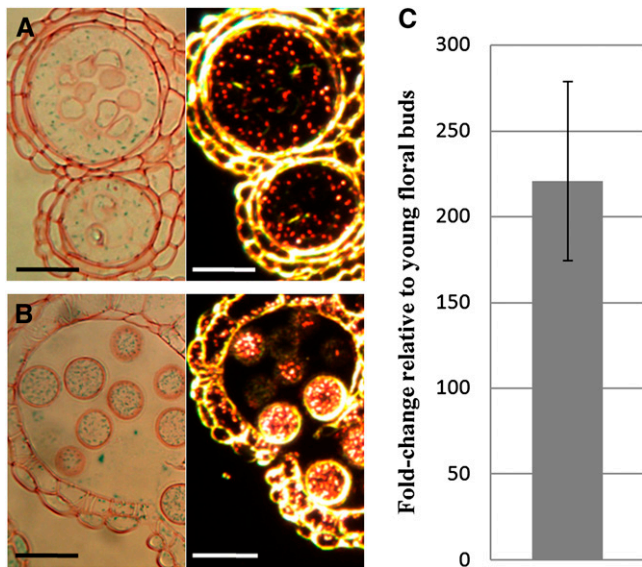


Figure 7. *GLOX1* Expression Analysis.

(A) and (B) Sections (3 μm) of *GLOX1* promoter:*GUS* anthers stained with safranin. Light and dark-field microscopy (GUS activity is visualized as red crystals) of a late stage 8 progressing to 9 (A) and stage 12 (B) anther. GUS crystals are present in the tapetum and developing pollen grains.

(C) Comparative qRT-PCR analysis of *GLOX1* transcript levels in wild-type mature (anther stages 10 to 12) versus young (anther stages ≤ 9) floral buds. The *GLOX1* transcript level is higher in mature floral buds. Error bar represents SD. Bars = 25 μm .

data indicated a correlation between the level of *UNDEAD* transcript and the severity of the male sterility phenotype.

Alexander's stain was used to determine pollen cytoplasmic viability (Figure 9D), with viable pollen staining red and pollen grains lacking cytoplasm staining green. Most of the siRNA-121 *undead* stage 10 and beyond anthers examined possessed reduced numbers of pollen grains when compared with the wild type, and the majority of pollen grains stained green. Mature siRNA-121 *undead* stage 13 anthers released only a few pollen grains. Scanning electron microscopy showed that of the few pollen grains released, the majority were morphologically abnormal and collapsed, the exine coat appearing deformed and irregular (Figures 9E and 9F) compared with the wild type (see Supplemental Figure 8 online).

Sections of *undead* floral buds were examined to identify changes in tapetal and microspore development (Figure 10). At stage 7, the tapetal cell layer in *undead* exhibited increased vacuolation, similar to changes seen in the *myb80* mutant (Li et al., 2007; Zhang et al., 2007). Stage 10 *undead* anthers had high levels of aborted microspores (Figure 10C), again resembling the *myb80* mutant. At anther stages 12 and 13, the septum and stomium cell layers break down as normal. However, the majority of pollen grains are collapsed, clump together, and are not released (Figure 10D).

To determine the possible localization of *UNDEAD*, the peptide sequence was analyzed using TargetP (<http://www.cbs.dtu.dk/>)

and iPSORT (<http://ipsort.hgc.jp/>), which are known to be $\sim 85\%$ accurate in signal peptide prediction (Emanuelsson and von Heijne, 2001). Both analyses identified the presence of a signal peptide (KTTMNFVFLFF) targeting *UNDEAD* to the mitochondria, in agreement with a previous study by Beers et al. (2004).

Apoptosis-Like PCD Occurs Prematurely in *myb80* and *undead* Tapetum and Pollen

PCD is believed to be responsible for tapetal degeneration (Parish and Li, 2010). This process is characterized by cellular condensation, mitochondria and cytoskeleton degeneration, nuclear condensation, and internucleosomal cleavage of chromosomal DNA. To investigate the nature of the tapetal breakdown in the *myb80* and *undead* mutants, TUNEL assays were performed on 6- μm transverse sections of paraffin-embedded wild-type, *myb80*, and siRNA #3 *undead* anthers. The TUNEL assay detects in situ DNA cleavage, a hallmark feature of apoptosis-like PCD, by enzymatically incorporating fluorescein-12-dUTP into the 3'-OH ends of fragmented DNA. Anther staging was based primarily on floral bud size and stages; however, key anther morphology traits that are unaffected in the *myb80* mutant, such as tetrad formation corresponding to anther stage 7 and tetrad release at stage 8, were also used as an indicator of anther developmental stages (Smyth et al., 1990; Bowman et al., 1991; Peirson et al., 1996; Sanders et al., 1999). In the *myb80* mutant, tapetal and microspore degeneration commences at stage 9, resulting in distorted morphology. In the determination of anther stages 9 to 11, floral bud size was a key indicator.

Analysis of the wild type at anther stage 9 where microspores first develop the pollen wall (Figure 11A, arrow) failed to detect TUNEL signals in tapetal cells and microspores. However, TUNEL-positive signals were detected in the *myb80* tapetum at this stage (Figures 11G and 11H). Wild-type tapetal cells start to degenerate rapidly at anther stage 10 and are no longer detected at anther stage 12 (Sanders et al., 1999). During wild-type anther stage 10, the first observations of TUNEL signal in the tapetum were made, consistent with the findings of Vizcay-Barrena and Wilson (2006) (Figures 11C and 11D). TUNEL-positive signals in the *myb80* stage 10 anther became more prominent in the tapetal layer and also appeared in collapsing microspores (Figures 11I and 11J).

Anther dehiscence, characterized by breakage of the stomium, occurs during stage 13 of anther development. Pollen grains have reached maturity with the completion of pollen sexine development and mitotic divisions to generate the tricolpate pollen. In the *myb80* mutant (Figures 11K and 11L), TUNEL signal is clearly evident in the collapsed pollen and possibly in remnants of the tapetum among the cellular debris, whereas the wild-type pollen remains TUNEL negative (Figures 11E and 11F).

Premature PCD also occurs in the *undead* mutant anthers. Positive TUNEL signals first appear in stage 9 tapetum (Figures 12A and 12D). However, no TUNEL signal was detected in collapsed or the few morphologically normal microspores, consistent with the *myb80* TUNEL data for this stage. At stage 11, the remaining pollen grains appeared collapsed, and intense TUNEL signals were present in both the remnant tapetal cells and pollen

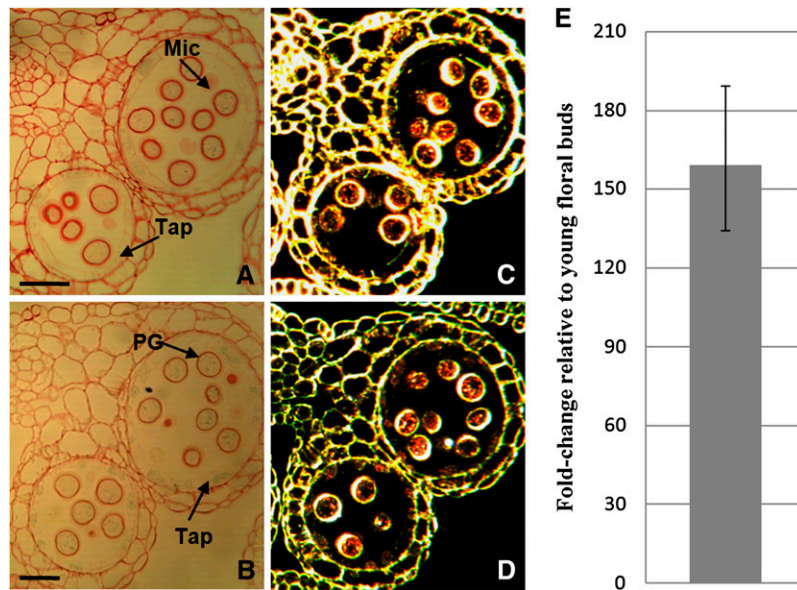


Figure 8. *VGD1* Expression Analysis.

(A) to (D) Sections (3 μm) of *VGD1* promoter:*GUS* anthers stained with safranin. Light microscopy of anthers at stages 10 (A) and 11 (B). Blue crystals are weakly present within the tapetum and developing pollen grains. Dark-field microscopy of anthers at stages 10 (C) and 11 (D). *GUS* activity is visualized as red crystals. *GUS* activity was not detected in stage 8 or earlier stages.

(E) Comparative qRT-PCR analysis of *VGD1* transcript levels in wild-type mature (anther stages 10 to 12) versus young (anther stages ≤ 9) floral buds. The *VGD1* transcript level is higher in mature floral buds. Error bar represents SD. Mic, microspores; Tap, tapetum; PG, pollen grain. Bars = 25 μm .

grains (Figures 12B and 12E). At stage 12, the *undead* anther locule contains collapsed pollen grains also undergoing PCD (Figures 12C and 12F).

DISCUSSION

MYB80 is essential for pollen development. In the *myb80* mutant, tapetal cell vacuolation and breakdown are premature and the small oil bodies, plastids, and vesicles are absent (Higginson et al., 2003; Li et al., 2007; Zhang et al., 2007). Tetrad callose dissolution is greatly reduced and the few microspores produced lack exine (Zhang et al., 2007). The *AMS* gene, which is expressed in the tapetum post microspore meiosis, does not appear to be part of the *MYB80* pathway (Xu et al., 2010). Microarray analysis of the *ms1* and *ams* buds in comparison to the wild type identified 260 and 549 differential expressed genes, respectively (Yang et al., 2007; Xu et al., 2010). Our transcriptome analysis identified 404 differentially expressed genes in young anthers of the *myb80* mutant compared with the wild type. The *myb80* mutant microarray shares 30 and 66 genes with the *ms1* and *ams* microarrays, respectively (see Supplemental Tables 3 and 4 online). Based on transcript analysis, Zhang et al. (2007) suggested that *MS1*, *MS2*, and the putative callase *A6* act downstream of MYB80. However, our ChIP analysis does not support direct regulation. In the *ams* mutant, vacuolation increases in the tapetal cells, which enlarge (hypertrophy) until they fill the vacuole (Sorensen et al., 2003). In the *ms1* mutant, abnormal vacuolation of tapetal cells also occurs. However, no

DNA fragmentation is detected in the tapetum (Vizcay-Barrena and Wilson, 2006). The *A6* gene plays a role in dissolution of the tetrad callose wall (Hird et al., 1993). Hence, blocking expression of the three genes previously shown to be downstream of *MYB80* does not result in phenotypes that fully resemble the *myb80* mutant. In particular, tapetal PCD is not premature.

The differential expression of genes in the *myb80* mutant might simply be a consequence of the premature tapetal degeneration. Consequently, we used the GR system to restore MYB80 function in the *myb80* mutant. Ito et al. (2007) used the same approach to study genes regulated by *MS1*. We selected 12 of the resulting differentially expressed genes based on their reported anther expression and obtained insertion mutants for them, but all anther phenotypes were identical to the wild type.

An additional 32 genes were then selected for ChIP analysis, again based on stamen-specific expression. The genes encoding the pectin methylesterase *VGD1*, *GLOX1*, and an A1 aspartic protease (*UNDEAD*) were positively enriched. EMSA confirmed that MYB80 binds to the promoters of all three genes with the motif CCAACC as the preferred binding site. *MS2*, *CYTOCHROME P450* (At1g01280), *A6*, and *MS1*, all genes involved in pollen development and expressed in the tapetum, were not enriched. Hence, they are not direct targets of MYB80.

VGD1 expression is absent or very weak in the tapetum when MYB80 is most active in anther stages 6 to 9, and the increase in *VGD1* expression correlates with the downregulation of *MYB80* expression at stage 10. *VGD1* encodes a pectin methylesterase homologous (PME) protein consisting of a PME inhibitor homologous domain, a pectinesterase homologous domain, and a

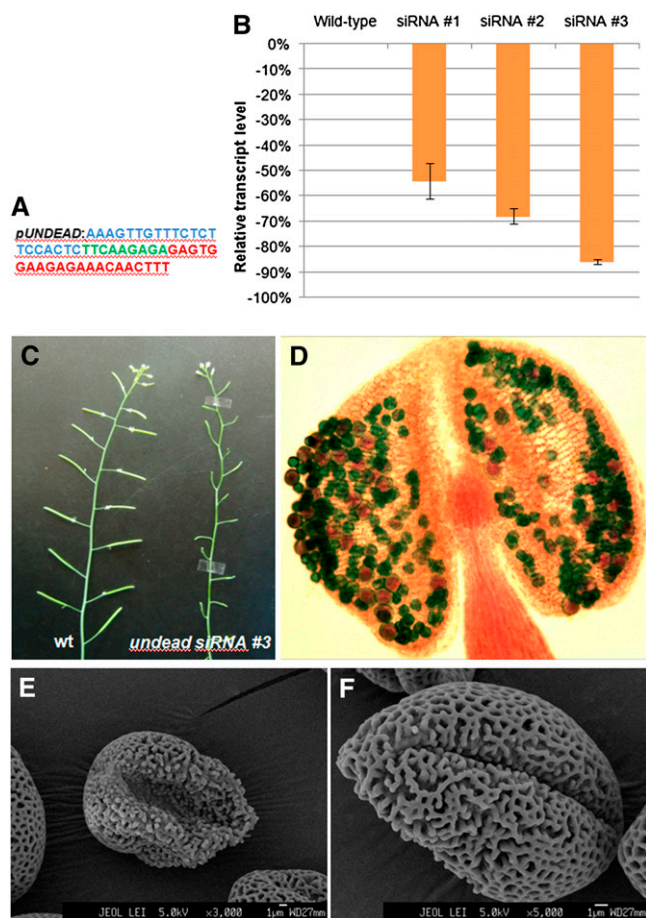


Figure 9. Functional Characterization of *UNDEAD* via siRNA-Mediated Gene Silencing.

(A) The siRNA construct consists of 21 nucleotides targeting the *UNDEAD* transcript at nucleotide position 121 (blue), a short 9-nucleotide loop (green), and the reverse complement 21 nucleotides (red). The siRNA was driven by the endogenous *UNDEAD* promoter.

(B) Real-time qPCR analysis of three different *undead* siRNA lines identified varying levels of transcript silencing. Error bars represent SD. Line #3 exhibited the greatest reduction of *UNDEAD* transcript.

(C) Silencing of *UNDEAD* transcript resulted in severe male sterility with line #3 displaying a near complete lack of silique elongation.

(D) Alexander's stain of an *undead* stage 12 anther shows a reduction in the number of pollen grains, the majority of which are collapsed and lacking viable cytoplasm (green staining).

(E) and **(F)** Scanning electron micrographs of *undead* pollen grains reveal irregularly shaped and collapsed grains with abnormal exine pattern formation. Wild-type pollen grain scanning electron micrograms are presented in Supplemental Figure 8 online.

secretion-related transmembrane domain (Jiang et al., 2005). PME are a group of cell wall-modifying enzymes that catalyze the demethylesterification of cell wall pectin (Jiang et al., 2005). The *vgd1* mutant exhibits partial male sterility, seed production being restricted to the top section of the mature siliques. Due to the specific expression in pollen and growing pollen tubes, *VGD1* may play a key role in strengthening the pollen tube cell walls,

thereby increasing the stability of the structure during growth (Jiang et al., 2005). Alternately, *VGD1* could be involved in modifying material released from the degenerating tapetum to form part of the pollen coat.

MYB80 may partially repress *GLOX1* transcription up to anther stages 8 to 9, and other transcription factors activate expression during the latter stages of pollen development. Overexpression of a *Vitis pseudoreticulata* *GLOX* can suppress powdery mildew hyphal development, possibly due to the generation of reactive oxygen species (ROS) (Guan et al., 2011). The authors suggest *Vp-GLOX* regulates cellular H_2O_2 levels since H_2O_2 can severely inhibit the enzyme. *Vp-GLOX* is a homolog of an *Arabidopsis* *GLOX* (At3g53950) whose function is unknown. The changes in and role of ROS during tapetum and pollen development are unclear. In plants, ROS may be a signaling molecule responsible for opening the permeability transition pore in mitochondria leading to PCD (Reape and McCabe, 2010). A homozygous *Arabidopsis glox1* insertion mutant could not be obtained for further study.

It appears that *At-MYB80* acts as both repressor and activator in the same tissue. Bifunctional transcription factors have been described previously in plants (Mena et al., 2002; Bossi et al., 2009; Ikeda et al., 2009). The nature of the promoter region of a gene and the binding of other factors may be involved in the conversion from repressor to activator.

The expression pattern of *UNDEAD* mirrors that of *MYB80* (Higginson et al., 2003; Li et al., 2007). A suitable insertion mutant was unavailable, so siRNA and amiRNA were used to down-regulate *UNDEAD* expression, and the degree of male sterility observed correlated with the reduction in *UNDEAD* transcript levels. Changes in the tapetal cells in anthers when the *UNDEAD* transcript levels were low resembled the *myb80* mutant, including increased tapetal vacuolation and premature cell death. *myb80* pollen grains appear to lack the exine (outer) layer (Zhang et al., 2007). Exine formation was also abnormal in the *undead* mutant but not to the extent of the *myb80* pollen. This is presumably because many of the genes downstream of *MYB80* are involved in lipid and sporopollenin synthesis (Zhang et al., 2007), and this is reflected by our *myb80* microarray analysis, as a large cluster of lipid synthesis and transport genes are affected.

DNA fragmentation is indicative of apoptosis-like PCD (Papini et al., 1999; Balk and Leaver, 2001; Love et al., 2008; Parish and Li, 2010). Using the TUNEL assay, we found that DNA fragmentation commences at stage 10 of wild-type tapetal cells. However, in the *myb80* mutant, TUNEL signal was first detected at anther stage 9 in tapetal cells. In the siRNA *undead* mutants, TUNEL signal also appeared in tapetal cells of anther stage 9. At stage 11, the signal was detected in remnant tapetal cells and collapsed pollen grains. The results are consistent with *MYB80* upregulation of *UNDEAD*, thereby delaying tapetal PCD, the program being initiated once *MYB80* and hence *UNDEAD* expression ceases. This differs from the *ms1* mutant where microspore and tapetal cells also collapse and degenerate; however, no DNA fragmentation is detected in the tapetum, suggesting necrotic breakdown rather than PCD is occurring (Vizcay-Barrena and Wilson, 2006).

Although *UNDEAD* gene expression ceases in the microspores of wild-type anthers at stage 11 as a consequence of a decrease in *MYB80* expression, unlike tapetal cells, the microspores do not undergo PCD. The PCD-inducing protein(s)

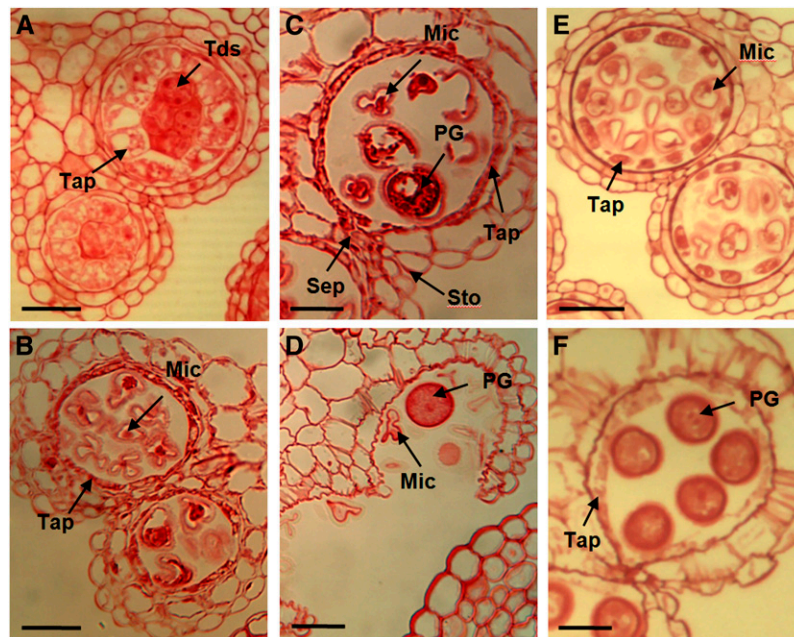


Figure 10. The *undead* Mutant Exhibits Premature Tapetal Degeneration.

Sections ($3\ \mu\text{m}$) of *undead* and wild-type anthers stained with safranin. MC, meiotic cell; Tap, tapetum; Tds, tetrads; Mic, microspores; PG, pollen grain; Sep, septum; Sto, stomium. Bars = $20\ \mu\text{m}$.

(A) Stage 7, tetrads are formed. The tapetum exhibits increased vacuolation similar to the *myb80* T-DNA mutant (Li et al., 2007).

(B) Stage 8, the tapetum appears sparse, exhibiting advanced degeneration commonly seen in wild-type stage 10 anthers.

(C) Stage 10, most of the microspores are aborted. A thin tapetal layer still remains.

(D) Stage 13, anther dehiscence and the breakage of both septum and stomium layers occur as normal. The collapsed pollen grains clump together and are not able to be released.

(E) Wild-type stage 8.

(F) Wild-type stage 11.

hydrolyzed by UNDEAD may no longer be expressed in microspores at this stage or perhaps UNDEAD is replaced by another protease. Alternately, the UNDEAD protein may persist in mature pollen grains while transcript has dissipated.

We conclude that MYB80 is delaying PCD by activating transcription of the *UNDEAD* gene. Proteases might be expected to activate rather than suppress PCD (Parish and Li, 2010); however, the *Arabidopsis* *PROMOTION OF CELL SURVIVAL1* (*PCS1*) gene also encodes an aspartic protease (Ge et al., 2005). *PCS1* is expressed in developing flowers and young siliques. Promoter:*GUS* analysis identified activity in anthers and pollen, but no information about tapetal expression was provided. Male and female gametophyte degeneration and excessive embryo apoptotic cell death prior to the torpedo stage occurred with a loss-of-function mutation. Anther dehiscence was blocked when *PCS1* was ectopically expressed using the 35S cauliflower mosaic virus promoter. The death of stomium and septum cells was prevented and leaf senescence was delayed.

Both UNDEAD and *PCS1* belong to the A1 family of *Arabidopsis* pepsin-like aspartic proteases (Beers et al., 2004). At the amino acid level, *PCS1* is only 27% similar to UNDEAD. Despite the differences, both *PCS1* and UNDEAD appear to regulate the timing of PCD. *PCS1* and UNDEAD both possess signal sequences; however, *PCS1* localization remains unclear, whereas the UNDEAD

signal sequence indicates the protein is directed to the mitochondria. Changes in mitochondrial outer membrane permeabilization and subsequent activation of cytoplasmic caspase proteases are responsible for apoptotic cell death in mammals (Tait and Green, 2010), but no caspase homologs have been found in plants (Sanmartin et al., 2005; Parish and Li, 2010). Release of apoptosis-inducing factor as a result of mitochondrial outer membrane permeabilization may contribute to caspase-independent cell death in mammals (Tait and Green, 2010). Vaux (2011) argues that cytochrome c is the only protein released from mitochondria for which there is strong evidence it is involved in mammalian cell death. Other proteins are released, some secondarily from the outer membrane by caspase activity, but evidence for a major role in cell death is lacking. A role for plant mitochondria has not yet been established. Cytochrome c is released from plant mitochondria by a variety of PCD-inducing stimuli, such as heat shock, D-mannose, menadione, and ceramide (Balk et al., 1999; Stein and Hansen, 1999; Sun et al., 1999; Reape and McCabe, 2008). The partial release of cytochrome c through transient pores in the mitochondrial membrane correlates with cytological abnormalities in tapetal cells of the Petiolaris-cytoplasmic male sterile (*PET1-CMS*) sunflower (*Helianthus annuus*; Balk and Leaver, 2001). However, purified cytochrome c added to plant mitochondria did not induce DNA fragmentation (Balk et al., 2003).

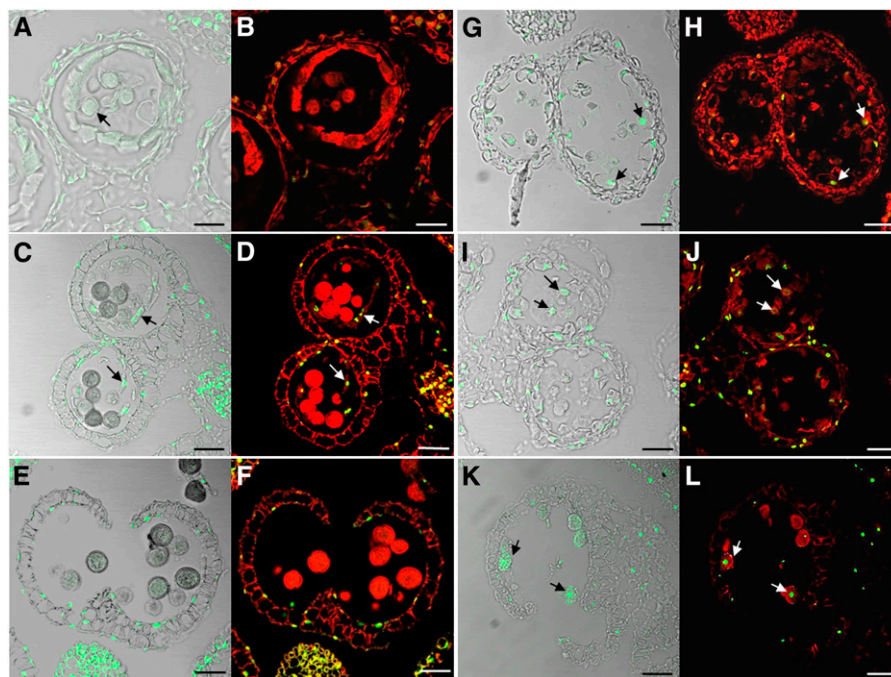


Figure 11. Tapetal PCD Occurs Prematurely in the *myb80* Mutant.

Confocal microscopy of DNA fragmentation detected using the TUNEL assay in 6- μ m sections of wild-type (**[A]** to **[F]**) and *myb80* (**[G]** to **[L]**) anthers. TUNEL-positive signal is indicated by the green fluorescence of fluorescein, and nuclei fluoresce deep red due to the counterstain propidium iodide. Bars = 25 μ m.

(A) and **(B)** Wild-type anther stage 9 with the first appearance of the pollen coat (arrow) was TUNEL-negative.

(C) and **(D)** TUNEL signal is first observed in the tapetum of wild-type anthers at stage 10 (arrows), which correlates with the onset of tapetal cell breakdown.

(E) and **(F)** At stage 13, the tapetum has degenerated completely, and TUNEL signal is visible only in the anther epidermis and endothecium.

(G) and **(H)** *myb80* anthers corresponding to stage 9 exhibit TUNEL signal in the tapetal layer but not in microspores (arrows).

(I) and **(J)** At stage 10 in *myb80*, TUNEL-positive signals appeared in the collapsing microspores (arrows).

(K) and **(L)** At stage 13 in *myb80*, TUNEL-positive nuclei are observed in the collapsed pollen (arrows).

Nonetheless, the possible mitochondrial location of UNDEAD indicates that the organelle may be involved in plant PCD.

UNDEAD may hydrolyze an apoptosis-inducing protein in the mitochondria that participates in PCD, either by being released into the cytoplasm or modifying mitochondrial outer membrane permeability. One function of MYB80 could be to induce transcription of the nuclear *UNDEAD* gene to ensure mitochondrial damage was prevented in tapetal cells. The downregulation of *MYB80* expression at stage 10 would shut down *UNDEAD* transcription and allow PCD to proceed. Such a model assumes a short half-life for the UNDEAD protein in mitochondria. A proposed model of MYB80 function is presented in Figure 13. The timing of tapetal PCD is critical for pollen development, and any delay or inhibition results in male sterility (Kawanabe et al., 2006). The *MYB80/UNDEAD* system may play a central role in this timing.

METHODS

Plant Materials and Growth

Arabidopsis thaliana accession Columbia (Col-0) was used for all gene transfer experiments and wild-type controls. Plants were grown on soil at

22°C under constant illumination or on germination medium containing the appropriate selective antibiotic. T-DNA insertion mutant lines were obtained from GABI-Kat (Max Planck Institute for Plant Breeding Research), the European Arabidopsis Stock Centre, and the ABRC. The insertion mutant lines used in this research are presented in Supplemental Table 1 online. Transgenic plants were transformed with *Agrobacterium tumefaciens* strain GV3101 by dripping of the *Agrobacterium* solution (40 mL of a 2-d culture resuspended in 20 mL of infiltration medium: 1 g sucrose, 6 μ L Silwet per 20 mL) onto each floret. One week later, the dripping procedure was repeated.

Plasmid Construction

Promoter:*GUS* constructs were generated by PCR amplification from genomic DNA. Fragments were cloned into the pENTR/D-TOPO Gateway vector (Invitrogen) and then cloned into pKGWFS7 using the LR clonase reaction. The AtMYB80:GR construct previously described by Li et al. (2007) was generated by PCR amplification of 1104 bp of the At-MYB80 promoter sequence and 1471 bp of the At-MYB80 coding sequence. This fragment was transcriptionally fused to 1.5 kb of the rat GR ligand gene using the restriction sites *Pst*I and *Spe*I then cloned into the pCambia 1380 vector (CAMBIA) using *Sal*I and *Spe*I restriction enzyme sites. The siRNA constructs were created by cloning the *UNDEAD* promoter into pCambia 1380 using *Bam*HI and *Hind*III restriction enzyme sites. Primer

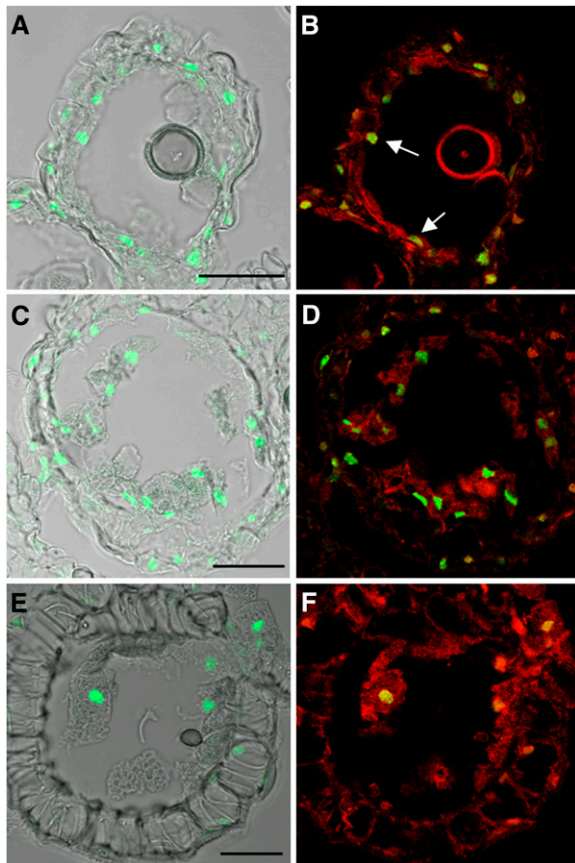


Figure 12. Tapetal PCD Occurs Prematurely in the *undead* Mutant.

Confocal microscopy of DNA fragmentation detected using the TUNEL assay in 8- μ m sections of siRNA *undead* anthers. TUNEL-positive signal is indicated by the green fluorescence of fluorescein. Grayfield (**[A]**, **[C]**, and **[E]**) and propidium iodide counterstain (**[B]**, **[D]**, and **[F]**) of stage 9 (**[A]** and **[B]**), 11 (**[C]** and **[D]**), and 12 anthers (**[E]** and **[F]**). TUNEL-positive signals are strongly present in stage 9 *undead* tapetum, suggesting that advanced PCD degeneration has occurred (arrows). TUNEL signal is present in collapsing microspores at stages 11 and 12. Bars = 25 μ m.

pairs (forward and reverse complement primers) were designed for each construct to incorporate 21 nucleotides targeting the *UNDEAD* transcript, a short 9-nucleotide loop, and the reverse complementary sequence of the 21-nucleotide target region. The primers also incorporated *Hind*III and *Spe*I restriction enzyme sites for cloning into pCambia 1380 containing the *UNDEAD* promoter. The At-MYB80 protein was expressed using *MYB80* cDNA cloned into the pRSETB (Invitrogen) vector at the *Kpn*I and *Hind*III sites. Primers are listed in Supplemental Table 5 online.

RT-PCR and qRT-PCR Analysis

Flower bud length was measured and staged according to Peirson et al. (1996). The anthers at stages 5 to 8 (0.4 to 0.9 mm) were dissected in RNAlater solution (Ambion). Total RNA was extracted from the isolated anthers using an RNeasy plant kit (Qiagen). First-strand cDNA synthesis was performed according to the manufacturer's instructions (Invitrogen Superscript III reverse transcriptase and reagents). The conditions for PCR amplification of cDNA were as follows: first cycle, 94°C for 3 min;

second cycle, 94°C for 30 s; 55°C for 30 s and 72°C for 50 s; third cycle, 72°C for 10 min. PCR products were visualized by running on a 1% agarose gel stained with ethidium bromide and captured digitally using a UV video capture system. qRT-PCR was performed using the iQ SYBR Green Supermix (Bio-Rad) on the MyiQ iCycler (Bio-Rad). The PCR conditions were as follows: 94°C for 3 min; 36 cycles of 94°C for 30 s; 51 to 56°C for 30 s; 72°C for 20 s; one cycle at 72°C for 5 min. Data were analyzed using the iQ5 (Bio-Rad) software, and differences in gene expression were calculated using the $2^{(-\Delta\Delta CT)}$ analysis method. Gene-specific primers are listed in Supplemental Table 5 online.

Sectioning of Resin-Embedded Floral Buds

Florets were fixed, embedded, and sectioned as described by Li et al. (2007).

Histochemical Assay of Transformed *Arabidopsis* Plants

Plant tissue was incubated in X-gluc solution at 37°C for 16 h. The chlorophyll was leached from the plant tissue with 70% ethanol. GUS staining was examined under a dissecting microscope. Determination of anther stage was based on bud measurements and stages of anther development described by Peirson et al. (1996) and reconciled with anther stages described by Sanders et al. (1999). Anthers were stained with Alexander's stain (Alexander, 1969) and examined microscopically.

Microarray Analysis

Approximately 1000 anthers at stages 5 to 8 were dissected from the wild type, *AtMYB80:GR* transgenic plants, and the *myb80* mutant for each biological replicate for subsequent RNA isolation. Each sample contained four biological replicates. To induce functional MYB80, plants were sprayed with 20 μ M DEX at the appropriate time prior to anther dissection. Total RNA was extracted from each collection of 1000 anthers using

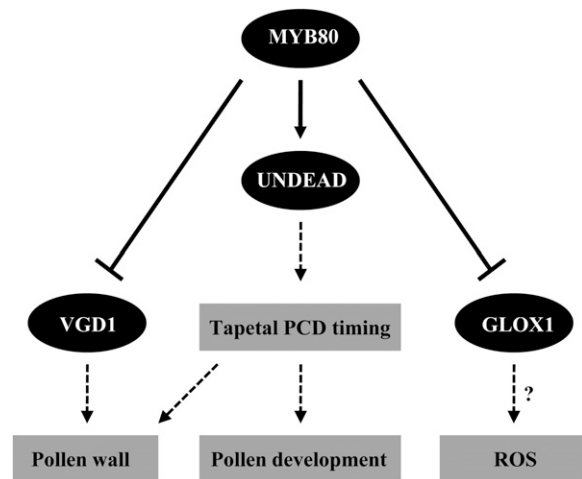


Figure 13. A Proposed Model of MYB80 Function in Tapetal and Pollen Development.

Solid lines represent direct gene regulation (arrows represent positive regulation and closed arrows represent negative regulation, respectively). Dashed lines represent function. ?, Hypothesized function. For a comprehensive model, see Wilson and Zhang (2009) and Parish and Li (2010).

the RNeasy plant kit (Qiagen). Microarray analysis was performed using 300 ng of total RNA per sample as described in the Genechip Expression Analysis Technical Manual (Affymetrix). Following biotin labeling of cRNA and fragmentation, samples were hybridized to Affymetrix *Arabidopsis* ATH1 genome arrays, washed using a Genechip fluidics station, and scanned using the Genechip Scanner 3000. Microarray data were processed using the ArrayAssist 5.5.1 software provided by Stratagene and Strand Life Sciences. The CEL files were analyzed with the PLIER algorithm, which provides background subtraction, normalization, and probe summarization. Variance stabilization was performed to add a fixed quantity (16) to all linear scale signal values, which suppresses noise at log signal values. Linear scale data were converted into log scale, where logs are taken to base 2. The log data set was then subjected to significance analysis (unpaired *t* test) to obtain a *P* value, a fold change, and a direction of change (up or down) for each gene. The Benjamini-Hochberg false discovery rate method was used to obtain *P* values corrected for multiple testing.

TUNEL Assay

Whole inflorescences were fixed in 4% (v/v) paraformaldehyde in PBS, 0.1% (v/v) Triton X-100, and 0.1% (v/v) Tween 20 for 1 h at room temperature under vacuum and then incubated in fresh fixative overnight at 4°C. Samples were washed with PBS, dehydrated in a graded ethanol series, and cleared in ethanol/histoclear (2:1, 1:1, and 1:2) for 1 h each and three times in 100% histoclear for 1 h each. Inflorescences were embedded in paraffin wax. Sections of 6 μm were cut using a Jung rotary microtome and attached to silane-coated slides. For the TUNEL assay, sections were deparaffinized with 100% xylene, dehydrated in a graded ethanol series, and permeabilized in proteinase K. Nick-end labeling of fragmented DNA was performed using the DeadEnd Fluorometric TUNEL system (Promega) according to the manufacturer's instructions. Slides were counterstained with 1 μg/mL of propidium iodide and mounted with SlowFade Gold antifade reagent (Invitrogen). Cover slips were sealed with clear nail varnish and slides stored at 4°C with a desiccant. Samples were analyzed under a fluorescence scanning confocal microscope (Leica TCS SP2) using excitation at 488 nm and emission at 509 nm to view the green fluorescence of fluorescein and a 538/617-nm excitation/emission spectrum to view the red fluorescence of propidium iodide. Merged images were generated using the ImageJ program (National Institutes of Health).

ChIP and Promoter Sequence Analysis

To use ChIP, a specific antibody to the target protein of interest is required. We decided not to create an MYB80 antibody as it may not be specific given the high sequence similarity within the MYB family or the epitope may not be accessible in planta. The anti-GR PA-516 (Upsate) antibody was used to enrich for the AtMYB80:GR protein/DNA complex. The ChIP experiment was performed using the protocol described by Saleh et al. (2008). *myb80* mutant plants containing the *AtMYB80:GR* transgene were sprayed with 20 μM DEX. Anthers or floral buds were harvested 24 h after DEX induction. PCR was performed using a standard GoTaq (Promega), 50 μL total reaction volume, and the following cycling parameters: first cycle, 94°C for 2 min; 36 cycles of 94°C for 30 s, 51°C for 30 s and 72°C for 40 s; and one cycle of 72°C for 2 min. To identify putative MYB binding motifs, ~600 bp of the 5' untranslated promoter region was analyzed using cis-PLACE (www.dna.affrc.go.jp).

EMSA

Recombinant MYB80 protein was purified using Ni-NTA Superflow columns (Qiagen) according to the manufacturer's protocol. EMSA was

performed using a nonradioactive protocol available on the website of the Hammer Lab (University of Michigan; <http://www.med.umich.edu/hammerlab/>) and the protocol described by Li and Parish (1995). Probes were labeled with digoxigenin via PCR using digoxigenin-labeled dUTP (Roche). Primers were designed to amplify a probe of 150 to 200 bp in length based on the promoter region, which was the target of the ChIP analysis. Protein-probe binding was performed using 400 ng total protein, 3 μL of 5× binding buffer (20 mM NaCl, 5 mM MgCl₂, 20 mM Tris, pH 8, 10% glycerol, 0.5 mM EDTA, and 0.5 mM DTT), 1 μL of poly d(I-C), and 1 to 4 μL of unlabeled competitor probe.

Scanning Electron Micrograph

Scanning electron microscopy was performed as described by Li et al. (2007).

Accession Numbers

Sequence data from this article can be found in the Arabidopsis Genome Initiative or GenBank/EMBL databases and are presented in Table 1 (gene ID/locus) or Supplemental Table 1 online (T-DNA insertions).

Supplemental Data

The following materials are available in the online version of this article.

Supplemental Figure 1. RT-PCR Analysis to Validate the Microarray Data.

Supplemental Figure 2. RT-PCR Analysis to Validate the Inducible Microarray Data.

Supplemental Figure 3. ChIP Assay Using Floral Buds as Input Material.

Supplemental Figure 4. ChIP Assay Using Dissected Anthers (Stages 5 to 8) as Input Material.

Supplemental Figure 5. Recombinant MYB80 Protein Expression and Purification.

Supplemental Figure 6. Comparative qRT-PCR Analysis of *MYB80* Transcript Levels in Wild-Type Mature (Anther Stages 10 to 12) versus Young (Anther Stages ≤ 9) Floral Buds.

Supplemental Figure 7. Promoter:*GUS* Expression Analysis.

Supplemental Figure 8. Scanning Electron Micrograph of Wild-Type *Arabidopsis* Pollen Grain.

Supplemental Table 1. Summary of T-DNA Insertion Mutants Analyzed for Phenotypic Changes in Male Fertility.

Supplemental Table 2. Genes Identified to Be Differentially Expressed 24 h after Dexamethasone Induction of Functional MYB80 Compared with Noninduced and *myb80* Mutant.

Supplemental Table 3. List of Overlapping Genes (30) Present in Both the *ms1* (Yang et al., 2007) and *myb80* Microarray Data Set.

Supplemental Table 4. List of Overlapping Genes (66) Present in Both the *ams* (Xu et al., 2010) and *myb80* Microarray Data Set.

Supplemental Table 5. Primer Sequences Used in This Article.

Supplemental Data Set 1. Microarray Analysis of *myb80* versus Wild-Type Anthers at Stages 5 to 8.

ACKNOWLEDGMENTS

We thank Edgar Sakers (La Trobe University) for his hand-sectioning skills and technical help, Tracie Webster and Nga Nguyen (Victorian

AgriBiosciences Center) for their assistance with the Microarray Fluidics Station/Scanner, and Alexander Fink and Tim Brown (La Trobe University) for the introductory lesson on using the scanning electron and confocal microscopes. Part of this research was funded by an Australian Research Council Linkage Grant and a Grains Research and Development Corporation Support Grant to R.W.P.

AUTHOR CONTRIBUTIONS

H.A.P. designed the research, performed the research, analyzed the data, and wrote the article. S.I. designed the research, performed the research, and wrote the article. S.F.L. designed the research and analyzed the data. R.W.P. designed the research and wrote the article.

Received January 9, 2011; revised May 18, 2011; accepted May 29, 2011; published June 14, 2011.

REFERENCES

- Aarts, M.G., Dirkse, W.G., Stiekema, W.J., and Pereira, A.** (1993). Transposon tagging of a male sterility gene in *Arabidopsis*. *Nature* **363**: 715–717.
- Abe, H., Urao, T., Ito, T., Seki, M., Shinozaki, K., and Yamaguchi-Shinozaki, K.** (2003). *Arabidopsis* AtMYC2 (bHLH) and AtMYB2 (MYB) function as transcriptional activators in abscisic acid signaling. *Plant Cell* **15**: 63–78.
- Abe, H., Yamaguchi-Shinozaki, K., Urao, T., Iwasaki, T., Hosokawa, D., and Shinozaki, K.** (1997). Role of *Arabidopsis* MYC and MYB homologs in drought- and abscisic acid-regulated gene expression. *Plant Cell* **9**: 1859–1868.
- Alexander, M.P.** (1969). Differential staining of aborted and nonaborted pollen. *Stain Technol.* **44**: 117–122.
- Balk, J., Chew, S.K., Leaver, C.J., and McCabe, P.F.** (2003). The intermembrane space of plant mitochondria contains a DNase activity that may be involved in programmed cell death. *Plant J.* **34**: 573–583.
- Balk, J., and Leaver, C.J.** (2001). The PET1-CMS mitochondrial mutation in sunflower is associated with premature programmed cell death and cytochrome c release. *Plant Cell* **13**: 1803–1818.
- Balk, J., Leaver, C.J., and McCabe, P.F.** (1999). Translocation of cytochrome c from the mitochondria to the cytosol occurs during heat-induced programmed cell death in cucumber plants. *FEBS Lett.* **463**: 151–154.
- Baranowskij, N., Frohberg, C., Prat, S., and Willmitzer, L.** (1994). A novel DNA binding protein with homology to Myb oncoproteins containing only one repeat can function as a transcriptional activator. *EMBO J.* **13**: 5383–5392.
- Beers, E.P., Jones, A.M., and Dickerman, A.W.** (2004). The S8 serine, C1A cysteine and A1 aspartic protease families in *Arabidopsis*. *Phytochemistry* **65**: 43–58.
- Bossi, F., Cordoba, E., Dupré, P., Mendoza, M.S., Román, C.S., and León, P.** (2009). The *Arabidopsis* ABA-INSENSITIVE (ABI) 4 factor acts as a central transcription activator of the expression of its own gene, and for the induction of *ABI5* and *SBE2.2* genes during sugar signaling. *Plant J.* **59**: 359–374.
- Bowman, J.L., Smyth, D.R., and Meyerowitz, E.M.** (1991). Genetic interactions among floral homeotic genes of *Arabidopsis*. *Development* **112**: 1–20.
- Chakravarthy, S., Tuori, R.P., D'Ascenzo, M.D., Fobert, P.R., Despres, C., and Martin, G.B.** (2003). The tomato transcription factor Pti4 regulates defense-related gene expression via GCC box and non-GCC box cis elements. *Plant Cell* **15**: 3033–3050.
- Emanuelsson, O., and von Heijne, G.** (2001). Prediction of organellar targeting signals. *Biochim. Biophys. Acta* **1541**: 114–119.
- Ge, X., Dietrich, C., Matsuno, M., Li, G., Berg, H., and Xia, Y.** (2005). An *Arabidopsis* aspartic protease functions as an anti-cell-death component in reproduction and embryogenesis. *EMBO Rep.* **6**: 282–288.
- Grotewold, E., Drummond, B.J., Bowen, B., and Peterson, T.** (1994). The *myb*-homologous *P* gene controls phlobaphene pigmentation in maize floral organs by directly activating a flavonoid biosynthetic gene subset. *Cell* **76**: 543–553.
- Gubler, F., Raventos, D., Keys, M., Watts, R., Mundy, J., and Jacobsen, J.V.** (1999). Target genes and regulatory domains of the GAMYB transcriptional activator in cereal aleurone. *Plant J.* **17**: 1–9.
- Guan, X., Zhao, H., Xu, Y., and Wang, Y.** (2011). Transient expression of glyoxal oxidase from the Chinese wild grape *Vitis pseudoreticulata* can suppress powdery mildew in a susceptible genotype. *Protoplasma* **248**: 415–423.
- Higginson, T., Li, S.F., and Parish, R.W.** (2003). *AtMYB103* regulates tapetum and trichome development in *Arabidopsis thaliana*. *Plant J.* **35**: 177–192.
- Hird, D.L., Worrall, D., Hodge, R., Smartt, S., Paul, W., and Scott, R.** (1993). The anther-specific protein encoded by the *Brassica napus* and *Arabidopsis thaliana* A6 gene displays similarity to beta-1,3-glucanases. *Plant J.* **4**: 1023–1033.
- Hsieh, K., and Huang, A.H.C.** (2007). Tapetosomes in *Brassica tapetum* accumulate endoplasmic reticulum-derived flavonoids and alkanes for delivery to the pollen surface. *Plant Cell* **19**: 582–596.
- Ikeda, M., Mitsuda, N., and Ohme-Takagi, M.** (2009). *Arabidopsis* WUSCHEL is a bifunctional transcription factor that acts as a repressor in stem cell regulation and as an activator in floral patterning. *Plant Cell* **21**: 3493–3505.
- Ito, T., Nagata, N., Yoshida, Y., Ohme-Takagi, M., Ma, H., and Shinozaki, K.** (2007). *Arabidopsis* MALE STERILITY1 encodes a PHD-type transcription factor and regulates pollen and tapetum development. *Plant Cell* **19**: 3549–3562.
- Ito, T., and Shinozaki, K.** (2002). The MALE STERILITY1 gene of *Arabidopsis*, encoding a nuclear protein with a PHD-finger motif, is expressed in tapetal cells and is required for pollen maturation. *Plant Cell Physiol.* **43**: 1285–1292.
- Jiang, L., Yang, S.L., Xie, L.F., Puah, C.S., Zhang, X.Q., Yang, W.C., Sundaresan, V., and Ye, D.** (2005). *VANGUARD1* encodes a pectin methylesterase that enhances pollen tube growth in the *Arabidopsis* style and transmitting tract. *Plant Cell* **17**: 584–596.
- Kawanabe, T., Ariizumi, T., Kawai-Yamada, M., Uchimiya, H., and Toriyama, K.** (2006). Abolition of the tapetum suicide program ruins microsporogenesis. *Plant Cell Physiol.* **47**: 784–787.
- Li, S.F., Higginson, T., and Parish, R.W.** (1999). A novel MYB-related gene from *Arabidopsis thaliana* expressed in developing anthers. *Plant Cell Physiol.* **40**: 343–347.
- Li, S.F., Iacuone, S., and Parish, R.W.** (2007). Suppression and restoration of male fertility using a transcription factor. *Plant Biotechnol. J.* **5**: 297–312.
- Li, S.F., and Parish, R.W.** (1995). Isolation of two novel *myb*-like genes from *Arabidopsis* and studies on the DNA-binding properties of their products. *Plant J.* **8**: 963–972.
- Love, A.J., Milner, J.J., and Sadanandom, A.** (2008). Timing is everything: Regulatory overlap in plant cell death. *Trends Plant Sci.* **13**: 589–595.
- Mena, M., Cejudo, F.J., Isabel-Lamonedá, I., and Carbonero, P.** (2002). A role for the DOF transcription factor BPBF in the regulation of gibberellin-responsive genes in barley aleurone. *Plant Physiol.* **130**: 111–119.
- Millar, A.A., and Gubler, F.** (2005). The *Arabidopsis* GAMYB-like genes,

- MYB33* and *MYB65*, are microRNA-regulated genes that redundantly facilitate anther development. *Plant Cell* **17**: 705–721.
- Morant, M., Jørgensen, K., Schaller, H., Pinot, F., Møller, B.L., Werck-Reichhart, D., and Bak, S.** (2007). CYP703 is an ancient cytochrome P450 in land plants catalyzing in-chain hydroxylation of lauric acid to provide building blocks for sporopollenin synthesis in pollen. *Plant Cell* **19**: 1473–1487.
- Papini, A., Mosti, S., and Brighigna, L.** (1999). Programmed-cell-death events during tapetum development of angiosperms. *Protoplasma* **207**: 213–221.
- Parish, R.W., and Li, S.F.** (2010). Death of a tapetum: A programme of developmental altruism. *Plant Sci.* **178**: 73–89.
- Peirson, B.N., Owen, H.A., Feldmann, K.A., and Makaroff, C.A.** (1996). Characterization of three male-sterile mutants of *Arabidopsis thaliana* exhibiting alterations in meiosis. *Sex Plant Reprod.* **9**: 1–16.
- Planchais, S., Perennes, C., Glab, N., Mironov, V., Inzé, D., and Bergounioux, C.** (2002). Characterization of cis-acting element involved in cell cycle phase-independent activation of *Arath*;CycB1;1 transcription and identification of putative regulatory proteins. *Plant Mol. Biol.* **50**: 111–127.
- Ramsay, R.G., Ishii, S., and Gonda, T.J.** (1992). Interaction of the Myb protein with specific DNA binding sites. *J. Biol. Chem.* **267**: 5656–5662.
- Reape, T.J., and McCabe, P.F.** (2008). Apoptotic-like programmed cell death in plants. *New Phytol.* **180**: 13–26.
- Reape, T.J., and McCabe, P.F.** (2010). Apoptotic-like regulation of programmed cell death in plants. *Apoptosis* **15**: 249–256.
- Sainz, M.B., Grotewold, E., and Chandler, V.L.** (1997). Evidence for direct activation of an anthocyanin promoter by the maize C1 protein and comparison of DNA binding by related Myb domain proteins. *Plant Cell* **9**: 611–625.
- Saleh, A., Alvarez-Venegas, R., and Avramova, Z.** (2008). An efficient chromatin immunoprecipitation (ChIP) protocol for studying histone modifications in *Arabidopsis* plants. *Nat. Protoc.* **3**: 1018–1025.
- Sanders, P.M., Bui, A.Q., Weterings, K., McIntire, K.N., Hsu, Y., Lee, P.Y., Truong, M.T., Beals, T.P., and Goldberg, R.B.** (1999). Anther developmental defects in *Arabidopsis thaliana* male-sterile mutants. *Sex. Plant Reprod.* **11**: 297–322.
- Sanmartín, M., Jaroszewski, L., Raikhel, N.V., and Rojo, E.** (2005). Caspases. Regulating death since the origin of life. *Plant Physiol.* **137**: 841–847.
- Scholl, R.L., May, S.T., and Ware, D.H.** (2000). Seed and molecular resources for *Arabidopsis*. *Plant Physiol.* **124**: 1477–1480.
- Smyth, D.R., Bowman, J.L., and Meyerowitz, E.M.** (1990). Early flower development in *Arabidopsis*. *Plant Cell* **2**: 755–767.
- Sorensen, A.M., Kröber, S., Unte, U.S., Huijser, P., Dekker, K., and Saedler, H.** (2003). The *Arabidopsis* *ABORTED MICROSPORES* (*AMS*) gene encodes a MYC class transcription factor. *Plant J.* **33**: 413–423.
- Stein, J.C., and Hansen, G.** (1999). Mannose induces an endonuclease responsible for DNA laddering in plant cells. *Plant Physiol.* **121**: 71–80.
- Sun, Y.L., Zhao, Y., Hong, X., and Zhai, Z.H.** (1999). Cytochrome c release and caspase activation during menadione-induced apoptosis in plants. *FEBS Lett.* **462**: 317–321.
- Sundaresan, V., Springer, P., Volpe, T., Haward, S., Jones, J.D., Dean, C., Ma, H., and Martienssen, R.** (1995). Patterns of gene action in plant development revealed by enhancer trap and gene trap transposable elements. *Genes Dev.* **9**: 1797–1810.
- Tait, S.W., and Green, D.R.** (2010). Mitochondria and cell death: Outer membrane permeabilization and beyond. *Nat. Rev. Mol. Cell Biol.* **11**: 621–632.
- Urao, T., Yamaguchi-Shinozaki, K., Urao, S., and Shinozaki, K.** (1993). An *Arabidopsis* myb homolog is induced by dehydration stress and its gene product binds to the conserved MYB recognition sequence. *Plant Cell* **5**: 1529–1539.
- Vaux, D.L.** (2011). Apoptogenic factors released from mitochondria. *Biochim. Biophys. Acta* **1813**: 546–550.
- Vizcay-Barrena, G., and Wilson, Z.A.** (2006). Altered tapetal PCD and pollen wall development in the *Arabidopsis* *ms1* mutant. *J. Exp. Bot.* **57**: 2709–2717.
- Wilson, Z.A., Morroll, S.M., Dawson, J., Swarup, R., and Tighe, P.J.** (2001). The *Arabidopsis* *MALE STERILITY1* (*MS1*) gene is a transcriptional regulator of male gametogenesis, with homology to the PHD-finger family of transcription factors. *Plant J.* **28**: 27–39.
- Wilson, Z.A., and Zhang, D.B.** (2009). From *Arabidopsis* to rice: Pathways in pollen development. *J. Exp. Bot.* **60**: 1479–1492.
- Wu, S.S., Platt, K.A., Ratnayake, C., Wang, T.W., Ting, J.T., and Huang, A.H.** (1997). Isolation and characterization of neutral-lipid-containing organelles and globuli-filled plastids from *Brassica napus* tapetum. *Proc. Natl. Acad. Sci. USA* **94**: 12711–12716.
- Xu, J., Yang, C., Yuan, Z., Zhang, D., Gondwe, M.Y., Ding, Z., Liang, W., Zhang, D., and Wilson, Z.A.** (2010). The *ABORTED MICROSPORES* regulatory network is required for postmeiotic male reproductive development in *Arabidopsis thaliana*. *Plant Cell* **22**: 91–107.
- Yang, C., Vizcay-Barrena, G., Conner, K., and Wilson, Z.A.** (2007). *MALE STERILITY1* is required for tapetal development and pollen wall biosynthesis. *Plant Cell* **19**: 3530–3548.
- Zhang, W., Sun, Y., Timofejeva, L., Chen, C., Grossniklaus, U., and Ma, H.** (2006). Regulation of *Arabidopsis* tapetum development and function by *DYSFUNCTIONAL TAPETUM1* (*DYT1*) encoding a putative bHLH transcription factor. *Development* **133**: 3085–3095.
- Zhang, Z.B., et al.** (2007). Transcription factor *AtMYB103* is required for anther development by regulating tapetum development, callose dissolution and exine formation in *Arabidopsis*. *Plant J.* **52**: 528–538.
- Zhu, J., Chen, H., Li, H., Gao, J.F., Jiang, H., Wang, C., Guan, Y.F., and Yang, Z.N.** (2008). *Defective in Tapetal development and function 1* is essential for anther development and tapetal function for microspore maturation in *Arabidopsis*. *Plant J.* **55**: 266–277.